ARTICLE
Journal of Cellular Biochemistry 114:1257–1270 (2013)

Journal of Cellular Biochemistry

Curcumin Inhibits Telomerase and Induces Telomere Shortening and Apoptosis in Brain Tumour Cells

Aik Kia Khaw,[1] M. Pradeepa Hande,[1] Guruprasad Kalthur,[1,2] and M. Prakash Hande[1,3*]

[1] *Genome Stability Laboratory, Department of Physiology, Yong Loo Lin School of Medicine, National University of Singapore, Singapore 117597, Singapore*

[2] *Department of Obstetrics and Gynaecology, Clinical Embryology, Kasturba Medical College, Manipal University, Manipal 576 104, India*

[3] *Tembusu College, National University of Singapore, Singapore 138598, Singapore*

ABSTRACT

Curcumin, a polyphenolic compound isolated from *Curcuma longa* (Turmeric) is widely used in traditional Ayurvedic medicine. Its potential therapeutic effects on a variety of diseases have long been known. Though anti-tumour effects of curcumin have been reported earlier, its mode of action and telomerase inhibitory effects are not clearly determined in brain tumour cells. In the present study, we demonstrate that curcumin binds to cell surface membrane and infiltrates into cytoplasm to initiate apoptotic events. Curcumin treatment has resulted in higher cytotoxicity in the cells that express telomerase enzyme, highlighting its potential as an anticancer agent. Curcumin induced growth inhibition and cell cycle arrest at G2/M phase in the glioblastoma and medulloblastoma cells used in the study. Gene and protein expression analyses revealed that curcumin down-regulated *CCNE1*, *E2F1* and *CDK2* and up-regulated the expression of *PTEN* genes resulting in growth arrest at G2/M phase. Curcumin-induced apoptosis is found to be associated with increased caspase-3/7 activity and overexpression of Bax. In addition, down-regulation of Bcl2 and survivin was observed in curcumin-treated cells. Besides these effects, we found curcumin to be inhibiting telomerase activity and down-regulating hTERT mRNA expression leading to telomere shortening. We conclude that telomerase inhibitory effects of curcumin underscore its use in adjuvant cancer therapy. J. Cell. Biochem. 114: 1257–1270, 2013.

KEY WORDS: CURCUMIN; CELL CYCLE ARREST; APOPTOSIS; TELOMERES AND TELOMERASE; GLIOBLASTOMA AND MEDULLOBLASTOMA

Curcumin [(1E,6E)-1,7-bis(4-hydroxy-3-methoxyphenyl)-1,6-heptadiene-3,5-dione] is a polyphenolic compound isolated from the rhizomes of *Curcuma longa*, a member of Zingeberacae family. Turmeric is a common ingredient of Indian curry powder and used as a colouring additive for mustard, yogurts, canned beverages and baked products. It is widely used in traditional Ayurvedic medicinal system as an antioxidant, antiseptic, analgesic and anti-inflammatory agent [Wilken et al., 2011]. Approximately 2–5% of turmeric is comprised of curcumin which is responsible for the yellow colour and majority of therapeutic effects [Chattopadhyay et al., 2004]. Earlier studies have shown that curcumin has cancer chemo-preventive [Sharma et al., 2005], anticancer [Sa and Das, 2008], antiangiogenic and antimetastatic properties [Yoysungnoen et al., 2006]. Therefore, it is considered to have potential clinical applications in treating cancer.

Both in vivo and in vitro studies conducted earlier have shown that curcumin suppresses the cancer cell proliferation through its diverse action on the growing cancer cells [Wilken et al., 2011]. Anticancer activity of curcumin is attributed to its effect on mitotic spindle and cell cycle progression [Liu et al., 2011; Lu et al., 2011], induction of apoptosis (both p53-dependent and -independent pathways) [Choudhuri et al., 2002; Gogada et al., 2011; He et al., 2011; Watson et al., 2010ab], inhibition of matrix metalloproteinases [Boonrao et al., 2010; Lu et al., 2010] and inhibition of angiogenesis [Lin et al., 2007; Perry et al., 2010].

A recent study by Mosieniak et al. [2012] has shown that curcumin induces autophagy and senescence in colon cancer cells. Curcumin-mediated increase in cell death is demonstrated to be mediated through inhibition of telomerase activity in human cancer cells [Ramachandran et al., 2002; Cui et al., 2006; Mukherjee Nee

The authors declare that they have no conflict of interests.

Grant sponsor: Academic Research Fund, Ministry of Education, Singapore; Grant numbers: T206B3108, WBS: 185-000-153-112; Grant sponsor: National Medical Research Council, Ministry of Health, Singapore; Grant number: NMRC/EDG/0052/2009.

*Correspondence to: M. Prakash Hande, Department of Physiology, Yong Loo Lin School of Medicine, National University of Singapore, Block MD9, 2 Medical Drive, Singapore 117597, Singapore. E-mail: phsmph@nus.edu.sg

Manuscript Received: 27 August 2012; Manuscript Accepted: 14 November 2012

Accepted manuscript online in Wiley Online Library (wileyonlinelibrary.com): 28 November 2012

DOI 10.1002/jcb.24466 • © 2012 Wiley Periodicals, Inc.

Chakraborty et al., 2007]. In the present investigation, we demonstrate the correlation between growth inhibition, cell cycle regulation, cell death and telomerase activity in curcumin-treated brain tumour cells. In addition, we report the progressive telomere shortening following long-term treatment with curcumin in tumour cells.

MATERIALS AND METHODS

CELL LINES AND CELL CULTURE

Human glioblastoma multiforme cells A172 (Japanese Collection of Research Bioresources, JCRB0228), KNS60, U251MG(KO) and medulloblastoma cells ONS76 (Institute for Fermentation, IF050357, IF050285 and IF050355, respectively) were obtained from Dr. Masao Suzuki, National Institute of Radiological Sciences, Chiba, Japan. The cells were cultured in DMEM supplemented with 10% foetal bovine serum and 2% penicillin/streptomycin. Early passage normal human fibroblast (Normal1) cells (GM03651, Coriell Cell Repositories, USA) were grown in Earle's salt MEM (Invitrogen, USA) supplemented with 15% FBS, MEM amino acids (Invitrogen), 10 mM MEM non-essential amino acids (Invitrogen), MEM vitamin solution (Invitrogen) and penicillin/streptomycin (100 U/ml). Telomerase immortalised human foreskin fibroblast cells, hTERT-BJ1 (Clonetech Laboratories, Inc., USA) were grown in 4:1 ratio of DMEM and medium 199 (Sigma–Aldrich, USA) and enriched with (10%) FBS, 200 mM L-glutamine, 100 mM sodium pyruvate and 100 U/ml penicillin/streptomycin (Thermo Fisher Scientific, USA). All cells were cultured at 37°C and 5% CO_2 in an incubator. Fresh medium was added after every 2 days and the cell density was kept below 80% confluence.

DRUG PREPARATION AND TREATMENT

Curcumin (Sigma–Aldrich) was dissolved in 100% dimethyl sulfoxide (DMSO) to get a stock solution of 100 mM concentration. Twenty-four hours after seeding, the cells were treated with curcumin for 48 h (short-term experiments) and 15 days (long-term experiments). For the experiment, 1 μl each of 0, 20, 40, 60, 80 and 100 mM of working solution was added to achieve drug concentration of 0, 20, 40, 60, 80 and 100 μM in each of cell culture.

CRYSTAL VIOLET ASSAY

The cytotoxic effect of curcumin on the brain tumour cells was assessed using crystal violet assay. Briefly, the cells treated with curcumin for 48 h were plated in a 6-well plate at a density of 0.2×10^6 cells/well. After 48 h, the cells were gently washed with 1× phosphate buffered saline (PBS) followed by incubation in crystal violet staining solution (Sigma–Aldrich; 0.75% crystal violet in 50% ethanol with 1.75% formaldehyde and 0.25% NaCl) at room temperature. After 15 min, the dye was aspirated gently and the 6-well plate was washed with 1× PBS to remove excess stain. Thereafter, 1.5 ml of SDS (1%) was added to each well and mixed evenly by placing on a rotator. Once the crystal violet is completely dissolved, absorbance was measured by reading the optical density at 595 nm using a microplate reader.

CURCUMIN TRAFFICKING IN CELLS

The cells were cultured on sterile coverslips which were placed in 6-well plates and treated with DMSO and curcumin for different time points at 2, 6, 8, 12, 24 and 48 h. Following treatment, coverslips with attached cells were placed on glass slides and observed under Axioplan 2 imaging fluorescence microscope (Carl-Zeiss, Germany) with filter sets for FITC, TRITC and DAPI to monitor the drug distribution in the cells.

SINGLE CELL GEL ELECTROPHORESIS (SCGE) ASSAY

Curcumin-induced DNA damage in cells was assessed using SCGE (comet) assay. For this, control and curcumin-treated cells were harvested by trypsinisation, washed in ice-cold 1× PBS and resuspended in Hank's balanced salt solution (HBSS) with 10% DMSO with ethylenediaminetetraacetic acid (EDTA). The cells were then suspended in 0.7% low melting point agarose and immediately transferred onto the comet slide pre-coated with 1% normal melting point agarose (Trevigen, USA). After the gel is solidified, the slides were immersed in lysis solution at 4°C for 1 h followed by an alkaline electrophoresis buffer (300 mM NaOH, and 1 mM EDTA, pH > 13) for 40 min to achieve unwinding of DNA. Slides were then subjected to electrophoresis at 25 V, 300 mA for 20 min at room temperature, washed with neutral buffer (500 mM Tris–HCL, pH 7.5) and stained with SYBR® green. Fifty randomly selected comets per sample were analysed using CometImager v3.4.6 (ISIS Metasystems, Germany).

CELL CYCLE ANALYSIS

Cells treated with DMSO or curcumin for 48 h were harvested by trypsinisation and washed with 1× PBS. The cells were then fixed in 70% ethanol and stained with propidium iodide/triton X-100 staining solution containing RNase A by incubating at 37°C for 30 min. Subsequently, samples were analysed by flow cytometry at 488 nm excitation λ and 610 nm emission λ. Ten thousand events per sample were collected and the data were analysed using WinMDI (Windows Multiple Document Interface) v2.8 software.

COLONY FORMATION ASSAY

Cells were harvested at 48 h after curcumin treatment and the viability was assessed by trypan blue dye exclusion method. From control and curcumin-treated groups, 2,000 cells were plated on 100 mm culture dish and kept in 37°C incubator with CO_2 for 10 days. Culture medium was changed once in every 3 days. On Day 10, culture medium was gently aspirated and washed with 1× PBS. To each dish 2 ml of crystal violet solution (1%) was added and kept at room temperature for 15 min. After aspirating the crystal violet solution, culture dishes were air-dried and the colonies were counted. This was further confirmed by dissolving the crystal violet solution by 1% SDS and measuring the absorbance of the resultant solution at 595 nm.

ANNEXIN V-FITC STAINING

Apoptotic cells were measured using Annexin V-Fluorescein isothiocyanate (FITC) labelled staining kit (Sigma–Aldrich). Unstained control, propidium iodide (PI) stained hydrogen peroxide (H_2O_2) treated cells (necrotic control), and FITC stained staurosporine treated cells (apoptotic control) were included in the

experiment. DMSO and curcumin-treated cells were stained with mixture of PI and FITC. Samples were then analysed using Becton Dickinson FACSCalibur™ flow cytometer. Approximately, 10,000 events per sample were collected and the data were analysed using WINMDI v2.8 software.

WESTERN BLOT ANALYSIS

Total proteins from control and curcumin-treated cells were isolated using 100 μl of ice-cold RIPA (radio-immunoprecipitation assay) buffer (1% non-idet P-40, 1% sodium deoxycholate, 0.1% SDS, 0.15 M NaCl, 0.01 M sodium phosphate, 2 mM EDTA, 50 mM sodium fluoride, 0.2 mM sodium vanadate and 100 U/ml aprotinin, pH 7.2) with complete protease inhibitor cocktail tablet (Roche Molecular Systems, USA). The samples were gently mixed for 45 min at 4°C followed by centrifugation at 14,000 rpm for 10 min to collect the supernatant in fresh tubes. Protein concentration was determined by Bradford assay (Bio-Rad, USA) taking bovine serum albumin as a standard. In each well, 45–60 μg of protein was loaded, 7.5–12% acrylamide gel was ran at 40 mA/gel, and transferred at constant voltage 100 V. Western blot analyses of Bcl2, p53, phosphorylated p53, p21, survivin, procaspase 8, procaspase 9, MDM2, cyclin B1, cdk1, PTEN and β-actin (Santa Cruz Biotechnology, USA) were performed using specific antibodies. Densitometry was carried out with Kodak Molecular Imaging Software.

REAL-TIME RT-PCR OF hTR AND hTERT mRNA EXPRESSION

Quantitative detection of hTERT and hTR mRNA was performed with the commercially available LightCycler® *TeloTAGGG* hTERT Quantification Kit (Roche, Switzerland) and LightCycler® *TeloTAGGG* hTR Quantification Kit (Roche, Switzerland) using LightCycler® instrument (Roche Molecular Systems, USA). Total RNA was extracted using RNeasy kit (Qiagen, USA) according to the manufacturer's instructions. RNA yield and purity were assessed by Nanodrop (ND-1000 Spectrophotometer). Total RNA (200 ng) was used to perform real-time reverse transcription polymerase chain reaction (real-time RT-PCR) for *hTR*, *hTERT* and porphobilinogen deaminase (*PBGD*) in separate reactions. Expression of *hTR* and *hTERT* was calculated on a standard curve constructed from the standards supplied with the kit. For quantification, *hTR* and *hTERT* values were normalised to those of *PBGD* and expressed as the ratio of *hTR* and *hTERT* mRNA copy numbers to *PBGD* mRNA copy number.

TELOMERIC REPEAT AMPLIFICATION PROTOCOL (TRAP)

Telomerase activity was detected using commercially available TRAPeze® XL Telomerase Detection Kit (Millipore, USA). All steps were carried out according to the manufacturer's instructions. Total protein was extracted from the cell pellet by incubating in CHAPS lysis buffer for 30 min on ice. Samples were spun at maximum speed at 4°C for 20 min to collect the supernatant. Protein quantification was carried out using Bradford method and 1.5 μg protein was treated with 1 μl/ml RNase inhibitor to eliminate RNase before performing PCR reaction. The fluorescence signals were measured according to fluorescein (Ex: 485 nm; Em: 535 nm) and sulforhodamine (Ex: 585 nm; Em: 620 nm) using fluorescence plate reader TECAN SpectraFluor Plus.

TERMINAL RESTRICTION FRAGMENT (TRF)

Telomere length analysis was performed with the *TeloTAGGG* Telomere Length Assay kit (Roche, Switzerland) according to the manufacturer's instructions. Genomic DNA harvested from 15-day curcumin-treated samples was digested using *Hinf* I and *Rsa* I restriction enzymes. Digested DNA was run on 0.8% agarose gel at 60 V and submerged in denaturation and neutralisation solutions before it was set up for Southern blot transfer. After Southern blotting, the membrane was cross-linked using UV rays and washed with 2× SSC salt solution. Hybridisation was performed by incubating membrane with DIG-labelled probe for 3 h. After washing off excess probe, anti-DIG alkaline phosphatase was incubated with the bound hybridisation probe on the membrane. Detection buffer and substrate were then added to the membrane for signal detection. Telomere restriction fragments on Southern blot nylon membrane were developed onto X-ray film for further image processing using Kodak Molecular Imaging Software.

STATISTICAL ANALYSIS

Statistical comparisons between and among the groups were made using two-way ANOVA, Student's *t*-test (two-tailed), and contingency tables analysis (m^2 test and Fisher's exact test) using Microsoft Excel 2003 (Microsoft Corporation, USA) and GraphPad Prism version 4.00 for Windows (GraphPad Software, USA, www.graphpad.com). The difference was considered to be statistically significant when $P < 0.05$.

RESULTS

DETERMINATION OF INHIBITORY CONCENTRATION (IC_{50}) OF CURCUMIN IN BRAIN TUMOUR CELLS

Cells were treated with different concentration of curcumin (from 0 to 100 μM) for 48 h. The crystal violet assay showed that curcumin treatment resulted in dose-dependent decrease in cell density (Fig. 1A). Curcumin treatment produced differential cytotoxic effect in the decreasing order of sensitivity in the following cells: hTERT-BJ1, KNS60, A172, U251MG(KO), ONS76 and Normal1. Among the brain tumour cells, KNS60 appears to be the most sensitive and ONS76 is the most resistant cell type to growth inhibition following curcumin treatment. Among the two normal cell types, telomerase negative Normal1 cells had highest IC_{50} of 90 μM, while the IC_{50} of hTERT-BJ1 cell was at 20 μM. Cell types expressing telomerase enzyme (all the brain tumour cells and hTERT-BJ1) had IC_{50} of <50 μM. This indicates that curcumin may potentially sensitise the cells that express telomerase enzyme such as cancer cells. For further experiments respective IC_{50} concentrations were used for each cell type.

EFFECT OF CURCUMIN TREATMENT ON CELL MORPHOLOGY AND CELL DENSITY

Morphology and density of cells treated with curcumin and DMSO (control) were studied by observing them under light microscope. Significant reduction in cell density and changes in morphology were observed in all the brain tumour cells treated with curcumin for 48 h compared to their corresponding DMSO control (Fig. 1B). DMSO treated cells showed an increase in cell density and proliferated

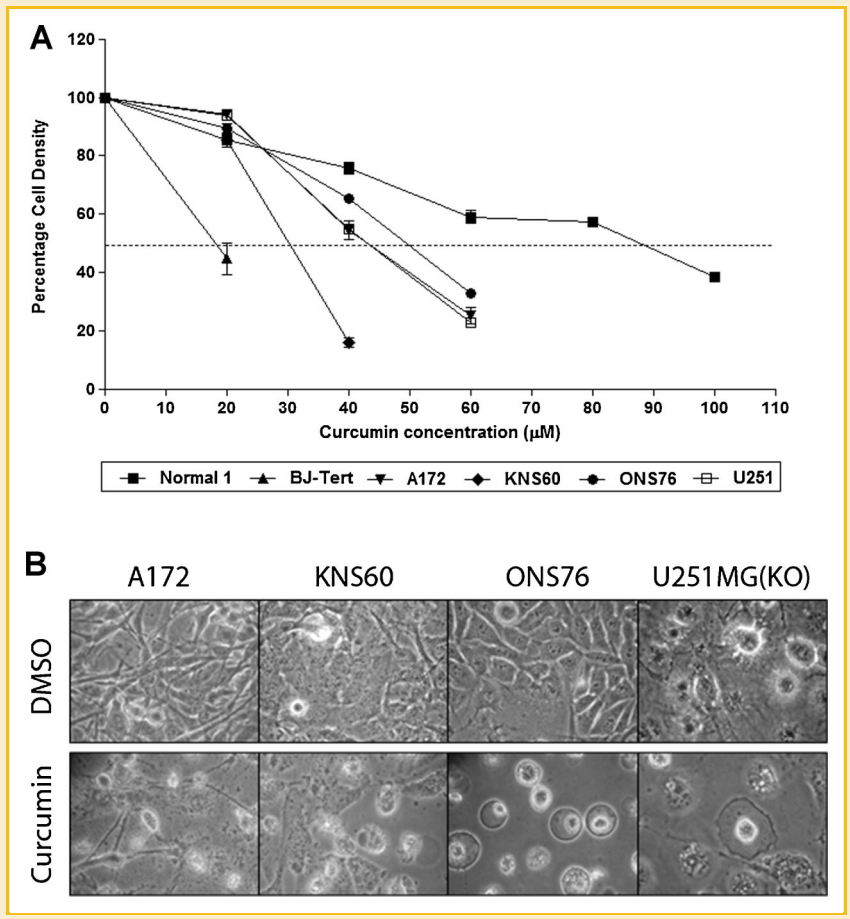

Fig. 1. A: Cell growth in different cell types following treatment with different concentrations of curcumin for 48 h as analysed by crystal violet assay. Telomerase negative Normal1 cells appear to be resistant to curcumin treatment. The IC_{50} values of telomerase positive cells relatively lower indicating higher sensitivity to curcumin. B: Brain tumour cell morphology at 48 h after treatment with curcumin. Curcumin treatment has exerted cytotoxic effect on all the cells resulting in lower cell density.

continuously indicating that DMSO does not induce any cell death or cell cycle arrest at this dose. However, curcumin-treated cells might have undergone certain degree of cell death and cell cycle arrest causing the cells to detach from the culture dish resulting in a lower cell density. In majority of the curcumin-treated cells, granulated and condensed cytoplasm was observed which is suggestive of apoptotic cell death (data not shown). In addition, vacuole associated phenotype resembling autophagy and enlarged or flattened cell morphology was observed in curcumin-treated ONS76 and U251MG(KO) cells, respectively.

CURCUMIN BINDS TO CELL SURFACE MEMBRANE AND POSSIBLY INDUCES CELL DEATH

The wavelength of fluorescent emission of curcumin was studied using UV–VIS scanning spectrophotometer (Shimadzu, Japan). At an excitation wavelength of 435 nm, curcumin generated maximal emission signal at 531 nm that corresponds to the green region in the UV–VIS spectra (Fig. 2A). Using this data, the route of curcumin trafficking into U251MG(KO) cells was investigated with the help of fluorescence microscope at different time points after curcumin treatment. The FITC filter was used to detect green fluorescence emitted by curcumin at 531 nm while the DAPI filter was used to detect blue fluorescence emitted by the cells due to autofluorescence. Curcumin was found to bind to the cell surface membrane at an early point and later infiltrated into cytoplasm, possibly leading to the induction of cell death (Fig. 2B).

CURCUMIN INDUCES G2/M PHASE ARREST AND CELL DEATH AND SUPPRESSES THE CLONOGENICITY OF CELLS

Curcumin and DMSO treated cells were stained with propidium iodide and subjected to FACS analysis. Curcumin-induced growth arrest of hTERT-BJ1, KNS60 and ONS76 at G2/M phase, while in Normal1, A172 and U251MG(KO) cells, it did not have any significant effect on the cell cycle. An increase in cell death was observed in KNS60 and ONS76 cells, which is evident from the increase in sub-G1 population. ONS76 cells had higher percentage of cell death compared KNS60 cells (Fig. 3A). These results show that although curcumin inhibited the growth of all of the three glioblastoma cell types and one medulloblastoma cell line, however, it only caused G2/M arrest in one of the three glioblastoma cell lines (KNS60) and the one medulloblastoma cell type (ONS76). Therefore, it appears that curcumin-induced growth inhibition in two of the three glioblastoma cell types [A172 and U251MG(KO)] may not be due to G2/M arrest.

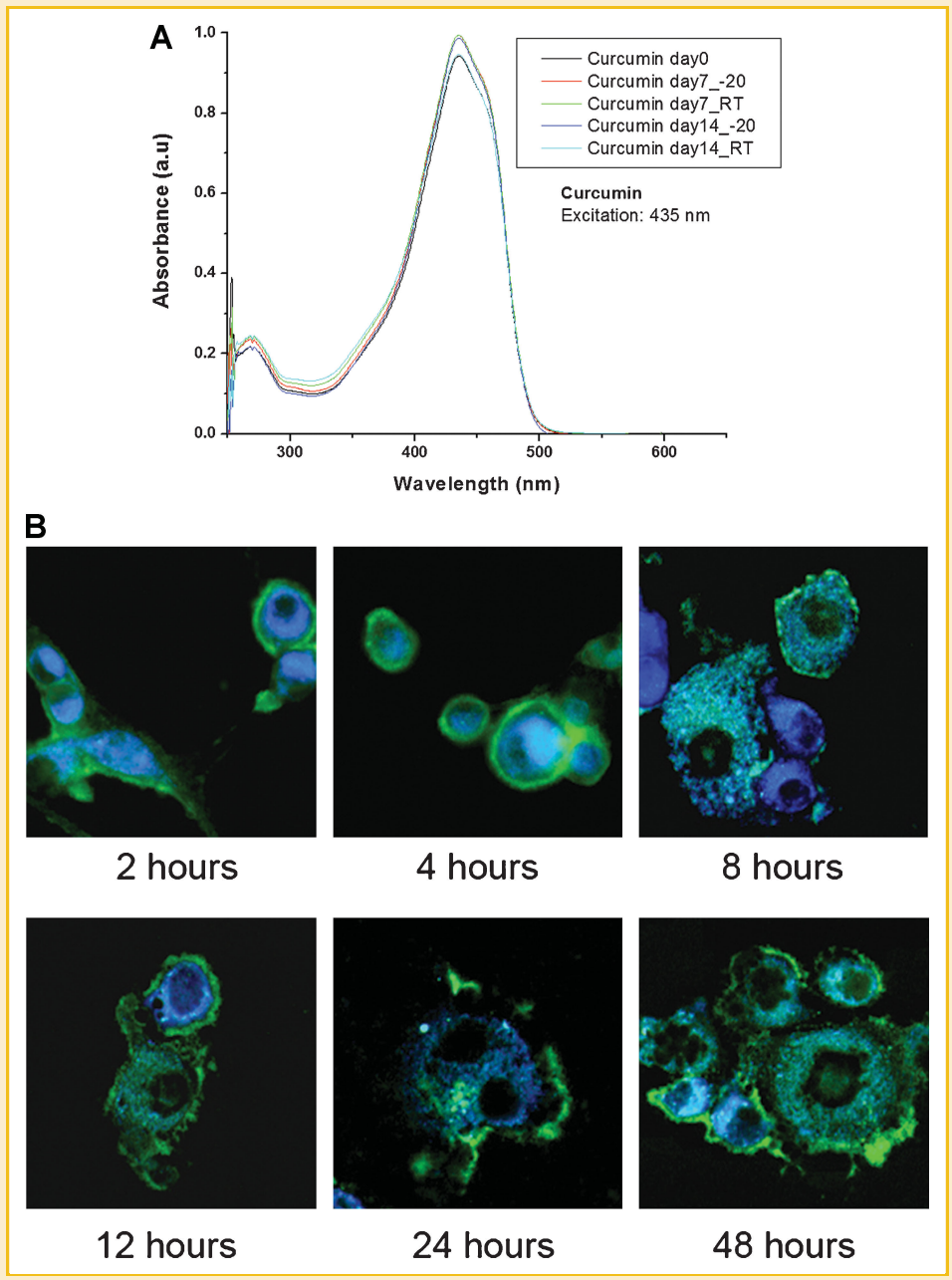

Fig. 2. A: Fluorescence spectra of curcumin. Absorbance values of curcumin stored at −20°C and room temperature were measured at Days 0, 7 and 14. B: Green fluorescence of curcumin in U251MG(KO) cells showing the route of drug trafficking. DNA staining is indicated by blue signal. Curcumin accumulates at the cell surface membrane and permeates into the cytoplasm to trigger the apoptotic cell death.

To study the long-term effect on the cell cycle arrest induced by curcumin, clonogenicity of the cells was studied. Cells were treated with curcumin for 48 h, after which 2×10^3 cells were reseeded and maintained in culture with drug-free medium for 10 days. A decreased colony number was observed in all curcumin-treated cell types compared to the respective DMSO controls (Fig. 3B).

Crystal violet assay suggested that KNS60 and ONS60 are more sensitive to cell killing after curcumin treatment. Surprisingly, A172 and U251MG(KO) displayed higher sensitivity in clonogenic assay (Fig. 3C). This clearly shows that curcumin may have differential effects on cells with different proliferative characteristics. In some cells, curcumin may elicit its effect following short-term exposure while in others it may induce long-term effects of cell death.

CURCUMIN-INDUCED CELL DEATH IS ASSOCIATED WITH DNA DAMAGE

A significant increase in caspase-3/7 activity following curcumin treatment was observed in all the cancer cell types (Fig. 4A). Highest caspase activity was observed in A172 cells at 24 and 48 h after curcumin treatment. To validate whether curcumin triggers

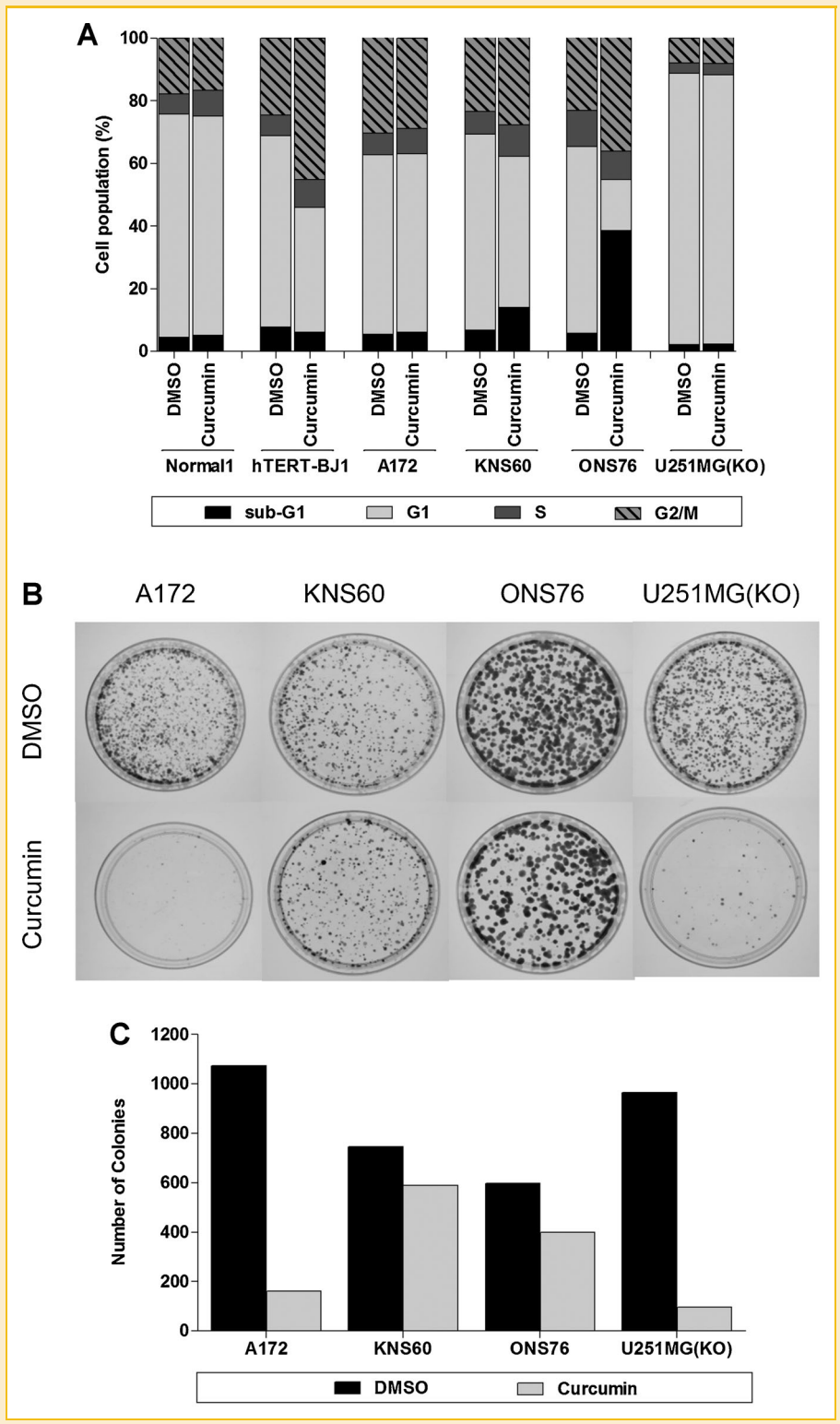

Fig. 3. A: Flow cytometry analysis of cell cycle profiles in curcumin-treated cells. Normal1, A172 and U251MG(KO) cells did not show significant changes in their cell cycle profiles indicating minimal response to curcumin. On the contrary, ONS76 cells showed a higher population in G2/M and sub-G1 region suggesting enhanced sensitivity to curcumin. Elevated sub-G1 cells were also seen in KNS60 cells. B: Growth inhibitory effect of curcumin as measured by colony formation assay in different cell types. Colony formation assay was done in 100 mm cell culture dish and cells seeded were allowed to grow for 10 days in the absence of curcumin. Colonies were stained with crystal violet for visualisation. C: Number of colonies in DMSO and curcumin-treated cells. Colonies were counted manually in at least three independent times and the results presented were represented in percentage in comparison with DMSO treated cells.

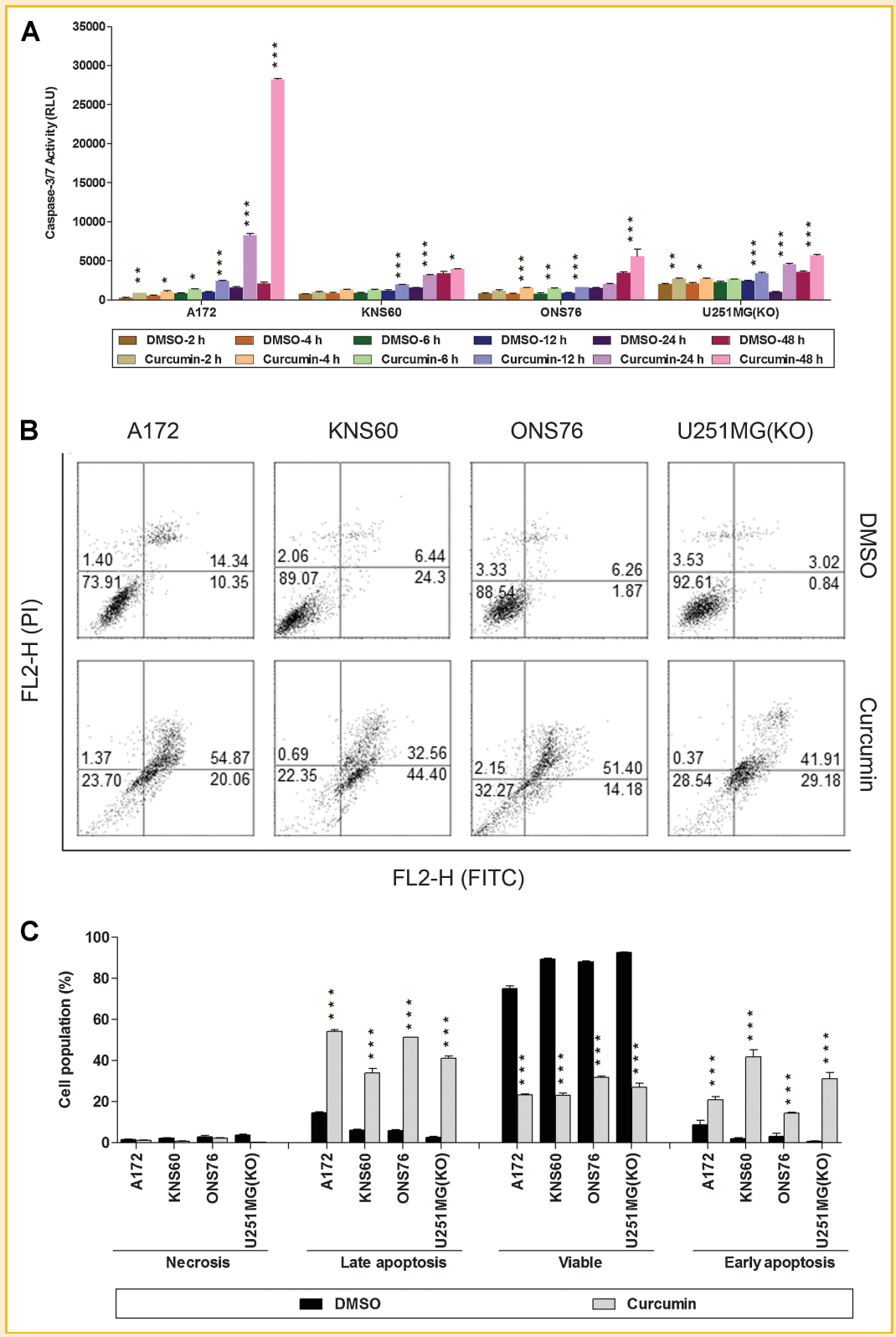

Fig. 4. A: Caspase-3/7 activity in brain tumour cells at different time intervals after curcumin treatment. $^{*}P < 0.05$, $^{**}P < 0.01$ and $^{***}P < 0.001$. B: Annexin V staining of curcumin-treated cells. Dot-plot data of FITC and PI staining measured by FACS analysis. C: Graphical representation of apoptotic and necrotic death in cells treated with curcumin. $^{***}P < 0.001$.

apoptotic cell death, annexin V staining was performed using FACS analysis. In support of earlier observation, all the cell types underwent apoptosis following curcumin treatment. A balanced population of early and late apoptotic cells was seen in most of the cell types except A172 and ONS76 cells, which had more cells at the late apoptotic region (Fig. 4B,C). This suggests that apoptosis is triggered immediately after curcumin treatment in A172 and ONS76 cells.

To determine whether curcumin induces DNA damage in the cell types used for the experiment, comet assay was performed. Curcumin treatment resulted in significant DNA damage in all the cell types studied. Interestingly, although curcumin treatment induced extensive DNA damage in Normal1 and A172 cells (Fig. 5A), there was no concomitant difference in cell cycle profile following curcumin treatment in these cells. It is possible that highly efficient DNA repair mechanism in Normal1 cells will allow them to continue growing while the damages are being repaired. On the contrary, the A172 cells may have a rather inefficient repair system that renders cells to undergo massive cell death that may occur after 48-h of curcumin treatment, especially when caspase activity increases preceding cell death. In other brain tumour cell types though the tail moments indicating DNA damage are not as high as that seen in Normal1 and A172, considerable amount of DNA was present in the tail region suggesting that curcumin-treated cells incurred more DNA damage than that of DMSO treated controls (Fig. 5B).

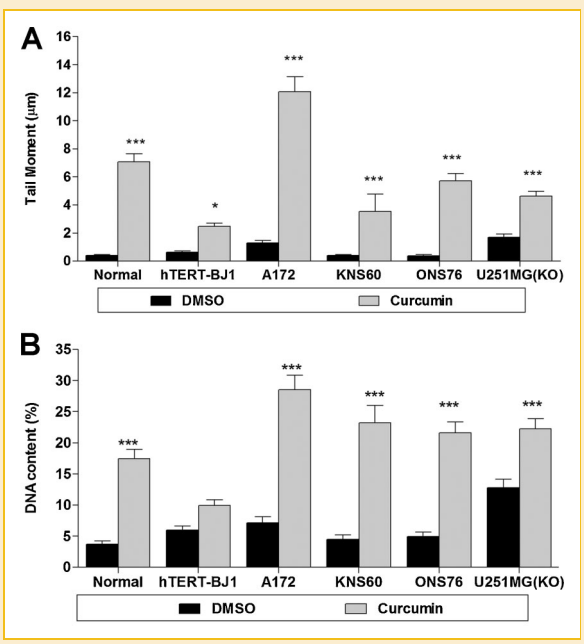

Fig. 5. DNA damage in cells treated with curcumin using comet assay. A: Degree of DNA damage in cells treated with curcumin represented by tail moment. A significant increase in DNA damage was observed in all the cell types with A172 cells exhibiting highest degree of damage. B: Graphical representation of DNA content in comet tails. $^{*}P < 0.05$ and $^{***}P < 0.001$.

CURCUMIN-INDUCED GROWTH ARREST AT G2/M PHASE CORRELATES WITH THE DOWN-REGULATION OF *CCNE1* AND *E2F1* GENES AND UP-REGULATION OF P21 PROTEIN

Expression of genes/proteins involved in cell cycle regulation was studied using Oligo GEArray® Cancer PathwayFinder and Western blotting respectively. As shown in Fig. 6A, decrease in the expression of *CCNE1*, *CDK2* and *E2F1* was observed in curcumin-treated cells. However, there was an up-regulation of *PTEN*, a negative regulator of cell survival factor AKT. Reduced *CCNE1* and *CDK2* genes that encode for cyclin E and cdk2 proteins, respectively, suggest that cells may get arrested at G1 phase of the cell cycle following curcumin treatment. In addition, down-regulation of *E2F* in all the brain tumour cells treated with curcumin further indicates that transcription of cyclins, cdks and checkpoint regulators is interrupted.

Western blot analysis of cell cycle regulatory proteins such as p53, p21, cyclin B1 and Cdk1 was performed following curcumin treatment. All the cell types exhibited a minimal difference in the expression of Cdk1 protein except ONS76 cells (Fig. 6B,C) which showed a significant decrease in the Cdk1 protein with concurrent increase in expression of p21. Decrease in Cdk1 and cyclin B1 proteins together with an increased p21 expression is very likely to have contributed to the arrest of ONS76 cells at G2/M phase at 48-h post-treatment. However, in the radioresistant KNS60 and U251MG(KO) cells, enhanced expression of cyclin B1 and decreased p21 expression were observed after curcumin treatment. The radiosensitive cells usually have high basal level of p53 expression, which was found to decrease following curcumin treatment in the present investigation. This confirms that KNS60 and U251MG(KO) cells were not arrested upon curcumin treatment. Altogether, the gene and protein expression profiles demonstrate that curcumin treatment resulted in cell cycle arrest in ONS76 cells and not in other cell types.

CURCUMIN TRIGGERS APOPTOTIC CELL DEATH BY OVEREXPRESSING BAX AND DOWN-REGULATING BCL2 AND SURVIVIN

To elucidate the cell death events triggered by curcumin, selected gene expression analysis of *BIRC5*, *TNFRSF10B* and *TNFRSF1A* was performed. Curcumin treatment up-regulated *BIRC5* that encodes for survivin protein, and *TNFRSF1A* which encodes for receptor for tumour necrosis factor (TNF) In all the brain tumour cells except A172 cells. However, the overexpression trends of these genes were either marginally above or below the threshold of the experiment suggesting that the changes in the regulation may not be significant. Most cells displayed a decrease in *TNFRSF10B* expression upon curcumin treatment (Fig. 7A). Down-regulation of this gene implies that the cells are less responsive to cell death induction by TNF.

To verify the cell death events induced by curcumin, Western blot analysis of selected death related proteins such as Bcl2, Bax, PARP1 and survivin was done (Fig. 7B,C). Contrary to mRNA levels, a decrease in survivin protein level was observed in all the brain tumour cells. Curcumin treatment also decreased the Bcl2 protein level as well indicating down-regulation of such antiapoptotic proteins. In addition, except for KNS60 cells, an increase in the expression of Bax, a proapoptotic protein was observed in all the

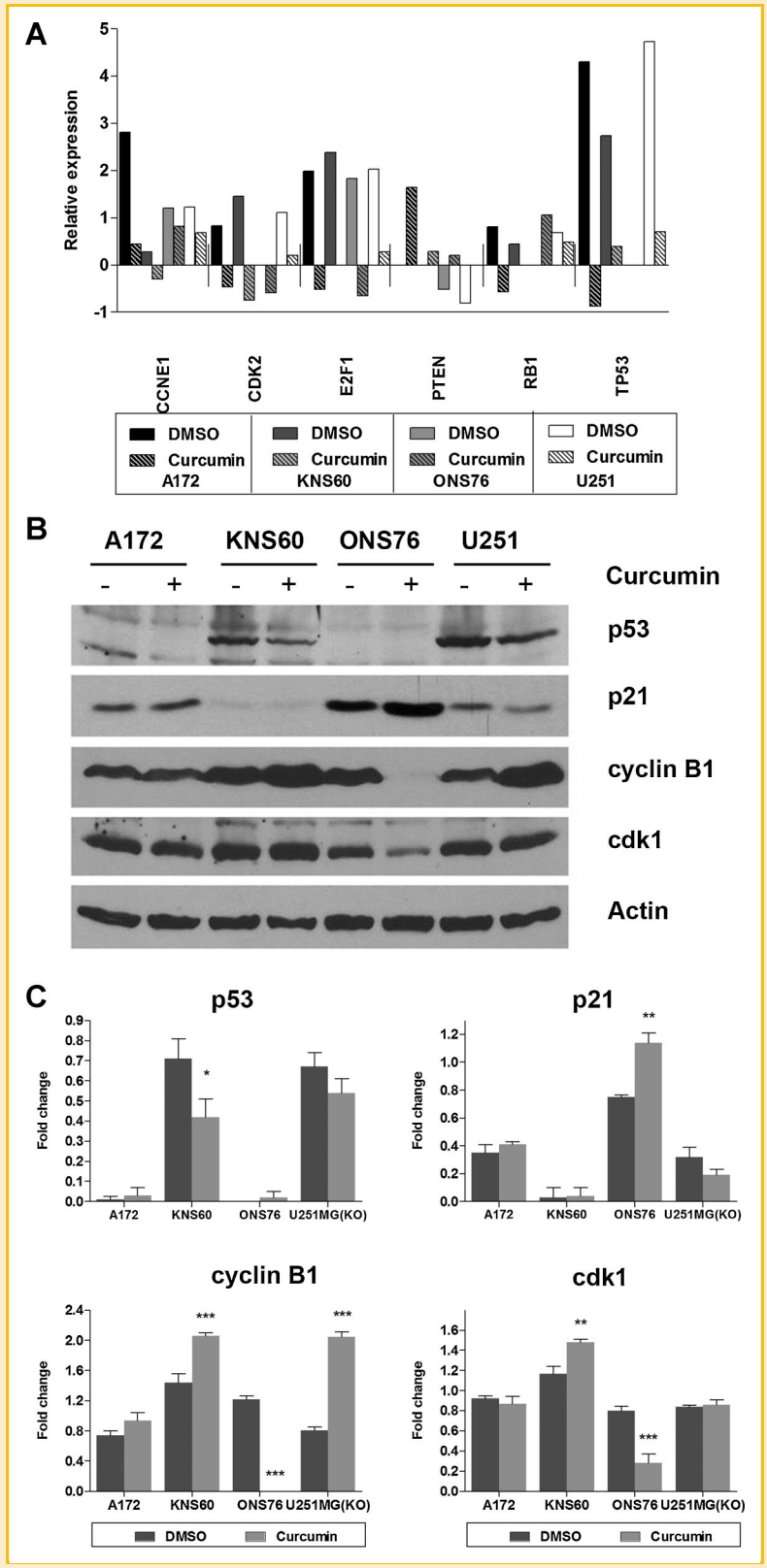

Fig. 6. A: Expression pattern of genes involved in cell cycle regulation performed using Oligo GEArray® Cancer PathwayFinder. Cell cycle regulator genes such as *CCNE1*, *CDK2*, *E2F1* and *PTEN* were analysed. Dotted red lines indicate the cut-off threshold at ±0.2. B: Western blot analysis of cell cycle regulatory proteins in brain tumour cells treated with curcumin. Blots were probed with specific antibodies. C: Fold change analysis of regulatory protein expressions by densitometry. $^{*}P < 0.05$ and $^{***}P < 0.001$.

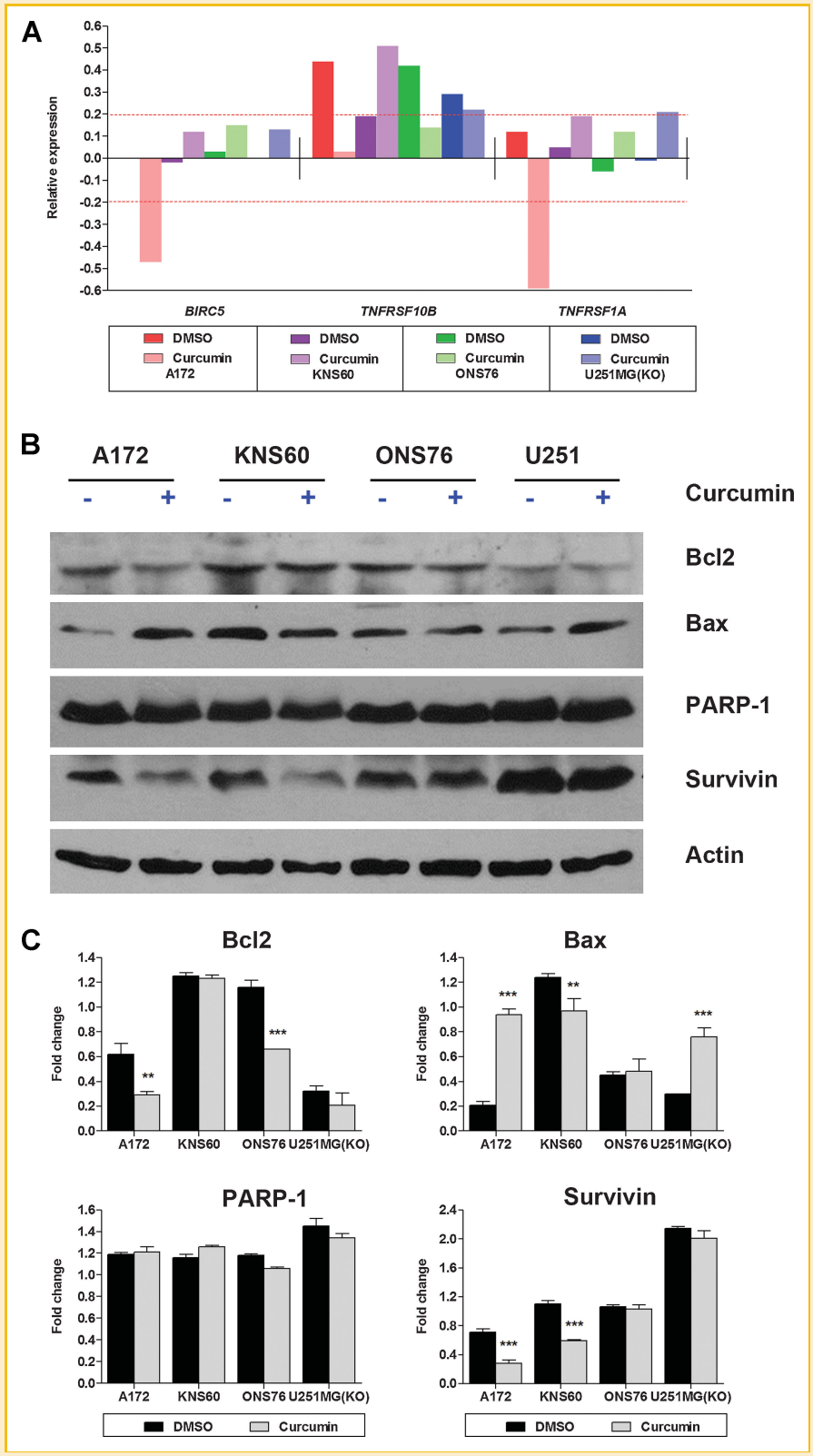

Fig. 7. A: Gene expression profile of cell death related genes *BIRC5*, *TNFRSF10B* and *TNFRSF1A* in curcumin-treated cells using Oligo GEArray® Cancer PathwayFinder. Red dotted lines indicate cut-off threshold at ±0.2. B: Western blot analysis of cell death related proteins. The blots were probed with specific antibodies. C: Fold change analysis of protein expressions by densitometry. $^{**}P < 0.01$ and $^{***}P < 0.001$.

other curcumin-treated cells. It is interesting to note that PARP1 did not show any significant change in its expression and, no cleaved PARP1 was detected in Western blotting. This finding shows that the apoptotic trigger induced by curcumin follows PARP1-independent pathway.

CURCUMIN INHIBITS TELOMERASE ACTIVITY BY DOWN-REGULATING *hTERT* mRNA EXPRESSION LEADING TO TELOMERE SHORTENING

The effect of curcumin on telomerase complex was studied using TRAP assay for telomerase activity and real-time RT-PCR analysis for *hTERT* and *hTR* mRNA expression levels. Telomere length in cells that had undergone long-term treatment with curcumin was measured using TRF assay. Telomerase activity was down-regulated after 48 h of curcumin treatment. Basal telomerase activity was high in KNS60 and ONS76 cells (Fig. 8A). In case of A172 and U251MG(KO) cells, though the basal telomerase activity was not as high, the percentage decrease in the enzyme activity after curcumin treatment was significant as was seen in KNS60 and ONS76 cells. This suggests that curcumin may have telomerase inhibitory effect on all the cancer cell types tested.

Relatively lower *hTERT* mRNA expression was observed in curcumin-treated cells compared to DMSO controls (Fig. 8B,C). DMSO controls were normalised across all samples to obtain a comparative fold change among the different cell types. In agreement with the results of the TRAP assay, KNS60 and ONS76 cells showed more than 50% decrease in the expression of *hTERT* mRNA. A172 and U251MG(KO) cells exhibited significant decrease in *hTERT* expression though not to the extent seen in the other two tumour cell types. On the other hand, data on *hTR* mRNA expression did not project a conclusive trend as that for the *hTERT* expression. Surprisingly, ONS76 and U251MG(KO) cells exhibited an increase in the expression of *hTR* mRNA upon curcumin treatment compared to A172 and KNS60 cells. These results suggest that the expression of *hTERT* may be associated with curcumin-induced telomerase inhibition.

To demonstrate the effectiveness of curcumin-induced telomerase inhibition, cells were treated with half the concentration of their respective IC_{50} for 15 continuous days with fresh medium. The drug was replenished every 48 h. All the cell types displayed a reduction in the mean telomere length following long-term treatment with curcumin (Fig. 8D,E). This decrease corresponded with curcumin-induced telomerase inhibition. KNS60 and ONS76 cells, which had inherently longer telomeres, exhibited drastic telomere shortening at the end of the long-term treatment. A172 and U251MG(KO) cells which had shorter basal telomere lengths, showed significant but modest telomere shortening following curcumin treatment.

DISCUSSION

In this study, various cellular and molecular responses of brain tumour cells to curcumin treatment were investigated. Curcumin-induced significant increase in cell death and DNA damage in all the cancer cell types studied. Earlier studies have reported the cytotoxic effects of curcumin in pancreatic, ovarian and lung cancer cells [Zheng et al., 2004; Lin et al., 2007; Sahu et al., 2009]. Interestingly, our data shows that telomerase negative human lung fibroblast cells exhibit higher IC_{50} with non-significant cell cycle arrest suggesting that non-cancerous cells may have better tolerance to the cytotoxic effects of curcumin.

Kunwar et al. [2008] have shown that the uptake and fluorescence intensity of curcumin was higher in normal cells compared to the tumour cells. Differential distribution of curcumin in membrane, cytoplasm and nuclear compartments of a cell with maximum localisation in the membrane was observed in breast cancer cells [Kunwar et al., 2008]. We observed initial accumulation of curcumin in the cell membrane, which later infiltrated into cytoplasm possibly initiating the apoptotic events. Data from annexin V staining and caspase-3/7 activity assay supported the observation of apoptotic cell death triggered by curcumin. In agreement with the earlier studies [Yang et al., 2010; Subramaniam et al., 2012], most of the cell types studied here displayed decreased expression of Bcl2 and survivin and increased expression of Bax following curcumin treatment. Additionally, curcumin is known to induce cell death events by inhibiting NFKB [Zheng et al., 2004; Duarte et al., 2010], activating death receptors [Bush et al., 2001], inducing ROS [Su et al., 2006; Thayyullathil et al., 2008] and mitochondrial hyperpolarisation [Cao et al., 2006, 2007]. Autophagy was also observed in cancer cells treated with curcumin [O'Sullivan-Coyne et al., 2009; Mosieniak et al., 2012].

Gene expression analysis showed that curcumin down-regulates *CCNE1*, *CDK2*, *E2F1* and up-regulates *PTEN* genes suggesting that cancer cells treated with curcumin may undergo cell cycle arrest and cease to proliferate. *PTEN* contributes to cell cycle regulation by inducing G1/S block and up-regulation of p27 which is recruited into the cyclin E/cdk2 complex. It has been demonstrated earlier that curcumin-induced cell cycle arrest and apoptosis is linked with increased expression of *CDK* inhibitors (p16, p21 and p27), and decreased expression of cyclin E and cyclin D1 in prostate cancer cells [Park et al., 2002; Srivastava et al., 2007]. Interestingly, we observed an increased expression of p21 and decreased expression of cyclin B1 and Cdk1 proteins after curcumin treatment in a radiosensitive ONS76 indicating cell cycle arrest. Whereas, radio-resistant cells [KNS60 and U251MG(KO)] presented somewhat different trend where p53 was down-regulated and cyclin B1 was up-regulated, suggesting resistance to cell cycle arrest following curcumin treatment. Collectively, we report for the first time that cells with different radiosensitivity exhibit differential response to curcumin treatment. Though expressions of certain cycle regulatory genes and proteins correlated with cell cycle arrest in two tumour cell types (KNS60 and ONS76), A172 and U251MG(KO) did not show this trend. This differential response could be due to the inherent different in their basal characteristics such as cell cycle timing, radiation sensitivity and telomere status. This needs further validation using other cell types with variable radiosensitivity.

Telomerase inhibitory effect of curcumin was reported earlier in breast cancer [Ramachandran et al., 2002], leukaemia [Chakraborty et al., 2006; Mukherjee Nee Chakraborty et al., 2007] and pancreatic cancer cells [Teng and Fahey, 2002]. We demonstrate here that curcumin suppresses telomerase activity in brain tumour cells which is associated with reduction in *hTERT* levels. The decreased

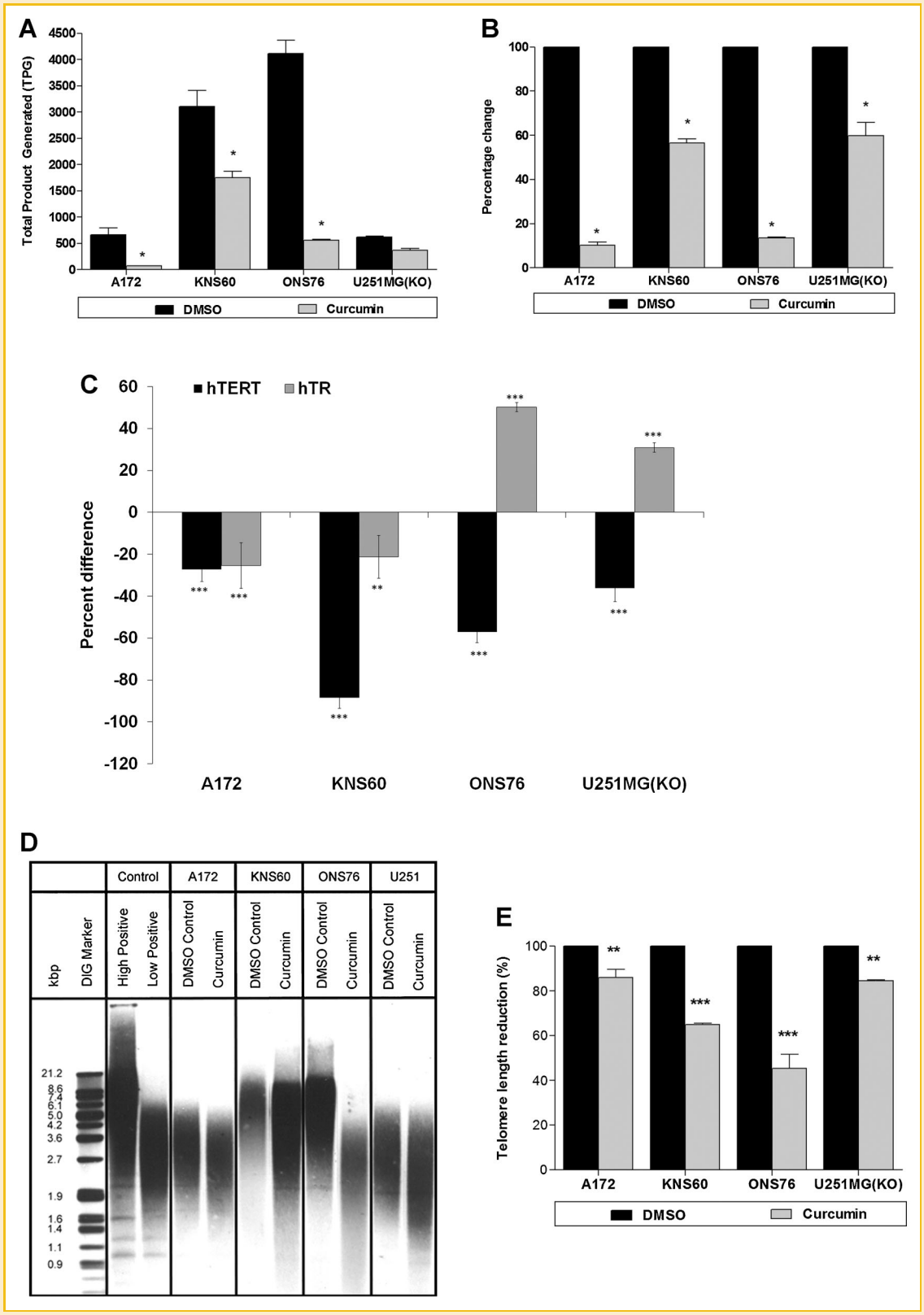

Fig. 8. Telomerase activity in curcumin-treated cells detected by Telomeric Repeat Amplification Protocol (TRAP) assay. A: Decrease in telomerase activity is represented by a reduction in the Total Product Generated (TPG). B: Representation of telomerase activity in percentage changes compared to telomerase positive control of the experiment. C: Real-Time RT-PCR results of *hTERT* and *hTR* mRNA expression of curcumin-treated cells. Fold changes of *hTERT* and *hTR* mRNA expression compared to DMSO control are presented. D: Analysis of telomere length of curcumin-treated cells using Terminal Restriction Fragment (TRF) assay. Telomeric probes were used to detect the telomeric region using Southern blot. Mean length was measured using a densitometer. E: Graphical representation of percentage changes in telomere length from Southern blot data. Fold change analysis of regulatory protein expressions by densitometry. $^{*}P < 0.05$, $^{**}P < 0.01$ and $^{***}P < 0.001$.

telomerase activity could be due to down-regulation of *hTERT* expression [Ramachandran et al., 2002; Cui et al., 2006; Mukherjee Nee Chakraborty et al., 2007] and/or suppression of the translocation of *hTERT* to the nucleus [Chakraborty et al., 2006; Lee and Chung, 2010] in *hTR*- or c-*Myc*-independent manner [Ramachandran et al., 2002]. We demonstrate that long-term curcumin treatment results in significant telomere shortening in brain tumour cells suggesting its potential clinical application as telomerase inhibitor. In conclusion, we propose that curcumin may selectively target cells that express telomerase enzyme, in turn making them more susceptible to curcumin-induced cytotoxicity. Importantly, our study reveals that action of curcumin is complex and diverse and its efficacy may depend on the cell types used in the study. Our long-term studies on brain tumour cells underscore the use of curcumin in adjuvant cancer therapy.

ACKNOWLEDGMENTS

GK was supported by Department of Biotechnology, Government of India, under Cutting Edge Research Enhancement and Scientific Training (CREST) fellowship.

REFERENCES

Boonrao M, Yodkeeree S, Ampasavate C, Anuchapreeda S, Limtrakul P. 2010. The inhibitory effect of turmeric curcuminoids on matrix metalloproteinase-3 secretion in human invasive breast carcinoma cells. Arch Pharm Res 33:989–998.

Bush JA, Cheung KJ, Jr., Li G. 2001. Curcumin induces apoptosis in human melanoma cells through a Fas receptor/caspase-8 pathway independent of p53. Exp Cell Res 271:305–314.

Cao J, Jia L, Zhou HM, Liu Y, Zhong LF. 2006. Mitochondrial and nuclear DNA damage induced by curcumin in human hepatoma G2 cells. Toxicol Sci 91:476–483.

Cao J, Liu Y, Jia L, Zhou HM, Kong Y, Yang G, Jiang LP, Li QJ, Zhong LF. 2007. Curcumin induces apoptosis through mitochondrial hyperpolarization and mtDNA damage in human hepatoma G2 cells. Free Radic Biol Med 43:968–975.

Chakraborty S, Ghosh U, Bhattacharyya NP, Bhattacharya RK, Roy M. 2006. Inhibition of telomerase activity and induction of apoptosis by curcumin in K-562 cells. Mutat Res 596:81–90.

Chattopadhyay I, Biswas K, Bandyopadhyay U, Banerjee RK. 2004. Turmeric and curcumin: Biological actions and medicinal applications. Curr Sci 87:1325–1325.

Choudhuri T, Pal S, Agwarwal ML, Das T, Sa G. 2002. Curcumin induces apoptosis in human breast cancer cells through p53-dependent Bax induction. FEBS Lett 512:334–340.

Cui SX, Qu XJ, Xie YY, Zhou L, Nakata M, Makuuchi M, Tang W. 2006. Curcumin inhibits telomerase activity in human cancer cell lines. Int J Mol Med 18:227–231.

Duarte VM, Han E, Veena MS, Salvado A, Suh JD, Liang LJ, Faull KF, Srivatsan ES, Wang MB. 2010. Curcumin enhances the effect of cisplatin in suppression of head and neck squamous cell carcinoma via inhibition of IKKbeta protein of the NFkappaB pathway. Mol Cancer Ther 9:2665–2675.

Gogada R, Amadori M, Zhang H, Jones A, Verone A, Pitarresi J, Jandhyam S, Prabhu V, Black JD, Chandra D. 2011. Curcumin induces Apaf-1-dependent, p21-mediated caspase activation and apoptosis. Cell Cycle 10:4128–4137.

He ZY, Shi CB, Wen H, Li FL, Wang BL, Wang J. 2011. Upregulation of p53 expression in patients with colorectal cancer by administration of curcumin. Cancer Invest 29:208–213.

Kunwar A, Barik A, Mishra B, Rathinasamy K, Pandey R, Priyadarsini KI. 2008. Quantitative cellular uptake, localization and cytotoxicity of curcumin in normal and tumor cells. Biochim Biophys Acta 1780:673–679.

Lee JH, Chung IK. 2010. Curcumin inhibits nuclear localization of telomerase by dissociating the Hsp90 co-chaperone p23 from hTERT. Cancer Lett 290:76–86.

Lin YG, Kunnumakkara AB, Nair A, Merritt WM, Han LY, Armaiz-Pena GN, Kamat AA, Spannuth WA, Gershenson DM, Lutgendorf SK, Aggarwal BB, Sood AK. 2007. Curcumin inhibits tumor growth and angiogenesis in ovarian carcinoma by targeting the nuclear factor-kappaB pathway. Clin Cancer Res 13:3423–3430.

Liu HS, Ke CS, Cheng HC, Huang CY, Su CL. 2011. Curcumin-induced mitotic spindle defect and cell cycle arrest in human bladder cancer cells occurs partly through inhibition of aurora A. Mol Pharmacol 80:638–646.

Lu DY, Leung YM, Cheung CW, Chen YR, Wong KL. 2010. Glial cell line-derived neurotrophic factor induces cell migration and matrix metalloproteinase-13 expression in glioma cells. Biochem Pharmacol 80:1201–1209.

Lu JJ, Cai YJ, Ding J. 2011. Curcumin induces DNA damage and caffeine-insensitive cell cycle arrest in colorectal carcinoma HCT116 cells. Mol Cell Biochem 354:247–252.

Mosieniak G, Adamowicz M, Alster O, Jaskowiak H, Szczepankiewicz AA, Wilczynski GM, Ciechomska I, Sikora E. 2012. Curcumin induces permanent growth arrest of human colon cancer cells: Link between senescence and autophagy. Mech Ageing Dev 133:444–455.

Mukherjee Nee Chakraborty S, Ghosh U, Bhattacharyya NP, Bhattacharya RK, Dey S, Roy M. 2007. Curcumin-induced apoptosis in human leukemia cell HL-60 is associated with inhibition of telomerase activity. Mol Cell Biochem 297:31–39.

O'Sullivan-Coyne G, O'Sullivan GC, O'Donovan TR, Piwocka K, McKenna SL. 2009. Curcumin induces apoptosis-independent death in oesophageal cancer cells. Br J Cancer 101:1585–1595.

Park MJ, Kim EH, Park IC, Lee HC, Woo SH, Lee JY, Hong YJ, Rhee CH, Choi SH, Shim BS, Lee SH, Hong SI. 2002. Curcumin inhibits cell cycle progression of immortalized human umbilical vein endothelial (ECV304) cells by up-regulating cyclin-dependent kinase inhibitor, p21WAF1/CIP1, p27KIP1 and p53. Int J Oncol 21:379–383.

Perry MC, Demeule M, Regina A, Moumdjian R, Beliveau R. 2010. Curcumin inhibits tumor growth and angiogenesis in glioblastoma xenografts. Mol Nutr Food Res 54:1192–1201.

Ramachandran C, Fonseca HB, Jhabvala P, Escalon EA, Melnick SJ. 2002. Curcumin inhibits telomerase activity through human telomerase reverse transcritpase in MCF-7 breast cancer cell line. Cancer Lett 184:1–6.

Sa G, Das T. 2008. Anti cancer effects of curcumin: Cycle of life and death. Cell Div 3:14.

Sahu RP, Batra S, Srivastava SK. 2009. Activation of ATM/Chk1 by curcumin causes cell cycle arrest and apoptosis in human pancreatic cancer cells. Br J Cancer 100:1425–1433.

Sharma RA, Gescher AJ, Steward WP. 2005. Curcumin: The story so far. Eur J Cancer 41:1955–1968.

Srivastava RK, Chen Q, Siddiqui I, Sarva K, Shankar S. 2007. Linkage of curcumin-induced cell cycle arrest and apoptosis by cyclin-dependent kinase inhibitor p21(/WAF1/CIP1). Cell Cycle 6:2953–2961.

Su CC, Lin JG, Li TM, Chung JG, Yang JS, Ip SW, Lin WC, Chen GW. 2006. Curcumin-induced apoptosis of human colon cancer colo 205 cells through the production of ROS, Ca2+ and the activation of caspase-3. Anticancer Res 26:4379–4389.

Subramaniam D, Ponnurangam S, Ramamoorthy P, Standing D, Battafarano RJ, Anant S, Sharma P. 2012. Curcumin induces cell death in

esophageal cancer cells through modulating Notch signaling. PLoS ONE 7:e30590.

Teng LS, Fahey TJ III. 2002. Can inhibition of telomerase increase pancreatic cancer cell's susceptibility to chemotherapeutic reagents? Hepatobiliary Pancreat Dis Int 1:155–160.

Thayyullathil F, Chathoth S, Hago A, Patel M, Galadari S. 2008. Rapid reactive oxygen species (ROS) generation induced by curcumin leads to caspase-dependent and -independent apoptosis in L929 cells. Free Radic Biol Med 45:1403–1412.

Watson JL, Greenshields A, Hill R, Hilchie A, Lee PW, Giacomantonio CA, Hoskin DW. 2010a. Curcumin-induced apoptosis in ovarian carcinoma cells is p53-independent and involves p38 mitogen-activated protein kinase activation and downregulation of Bcl-2 and survivin expression and Akt signaling. Mol Carcinog 49:13–24.

Watson JL, Hill R, Yaffe PB, Greenshields A, Walsh M, Lee PW, Giacomantonio CA, Hoskin DW. 2010b. Curcumin causes superoxide anion production and p53-independent apoptosis in human colon cancer cells. Cancer Lett 297:1–8.

Wilken R, Veena MS, Wang MB, Srivatsan ES. 2011. Curcumin: A review of anti-cancer properties and therapeutic activity in head and neck squamous cell carcinoma. Mol Cancer 10:12.

Yang J, Cao Y, Sun J, Zhang Y. 2010. Curcumin reduces the expression of Bcl-2 by upregulating miR-15a and miR-16 in MCF-7 cells. Med Oncol 27:1114–1118.

Yoysungnoen P, Wirachwong P, Bhattarakosol P, Niimi H, Patumraj S. 2006. Effects of curcumin on tumor angiogenesis and biomarkers, COX-2 and VEGF, in hepatocellular carcinoma cell-implanted nude mice. Clin Hemorheol Microcirc 34:109–115.

Zheng M, Ekmekcioglu S, Walch ET, Tang CH, Grimm EA. 2004. Inhibition of nuclear factor-kappaB and nitric oxide by curcumin induces G2/M cell cycle arrest and apoptosis in human melanoma cells. Melanoma Res 14:165–171.